DOI: 10.13009/EUCASS2019-661

8TH EUROPEAN CONFERENCE FOR AERONAUTICS AND AEROSPACE SCIENCES (EUCASS)

DOI:

Development of a MATLAB® Plume Impingement Tool for Fast System Analysis.

Pedro J. Herráiz⋆†, *José Mª Fernández*⋆ *and José R. Villa* ⋆
⋆*SENER, Ingeniería y Sistemas*
Severo Ochoa 4, 28760 Tres Cantos, Madrid, Spain
pedrojose.herraiz@sener.es · jm.fibarz@sener.es · jr.villa@sener.es
†Corresponding author

Abstract

Thrusters' plume interactions with spacecraft can have a very important impact in their different subsystems (thermal, power generation, GNC). Moreover, with the current trend of increasing the optical instruments, it is even more relevant to study its effects as a source of heat and contamination on the exposed components. It is also always relevant to determine the forces and torques that the impingement can induce on the overall spacecraft. Therefore, prediction of the plume impingement effects during the design phases is becoming more relevant in order to find the best geometrical system configuration and components accommodation.

There already exist different advanced tools based on computational fluid dynamics (CFD) and Direct Simulation Monte Carlo (DSMC) methods that allow performing detailed analysis. However, they are complex and time consuming, and could not be the best option to use during the preliminary design phases but in final phases to consolidate the results. In early stages of the design, there is needed to multiple configurations in a very short time to adapt the design to the constraints imposed by all the subsystems and several trade-offs need to be performed.

The present work intends to provide an efficient alternative approach that allows evaluating the plume impingement phenomenon in early design phases. An in-house developed tool implemented in MATLAB® is presented. This tool is based on the combination of different classical source flow methods (Simons-Boynton and Mayer-Hermel-Rogers), and free-molecular flow interactions with the surfaces. It allows performing fast and easy evaluations of the configuration changes in the spacecraft.

Based on the detailed plume flow results provided by the thrusters' supplier, a set of models' parameters correction is proposed to ensure the fit of the employed source model in order to have accurate results at a very low computational cost.

The developed tool has been employed in the design of Proba-3 ESA's IOD mission to determine the heat fluxes, contamination, power loss and disturbance forces of each spacecraft configuration allowing to evaluate the impact of the changes in the thrusters' orientations and positions and external elements.

1. Introduction

Each spacecraft that implements propulsive elements to perform control attitude or orbit management uses thrusters that have to be fired and generate an exhaust plume from the exit of the nozzle that may interact with the surfaces of the spacecraft generating undesired force and torque disturbances and other pernicious effects like heat fluxes or contamination effects. All this effects are the plume impingement associated problems and needs to be taken into account in the preliminary design phase of any mission to ensure that the required performances and contamination criteria are met[1].[2]

DOI: 10.13009/EUCASS2019-661

Since the first impingement analysis and simple models based on cosine source models that consider the nozzle as a point emitting particles that travels in straight line diverging radially,[3] a lot of developments has been done implementing corrections to the models either by adjusting the boundary layer[3,4] or adding other effects[5,6]. Even with this advances, the fitting of the results of the source models with the reality is limited and other approaches has been developed based on coupling of Navier-Stokes analysis for the continuum part with DSMC analysis for the free molecular flow part[7,8] or gaskinetic theory[9,10,11,12]. This approaches generate better results but its implementation is much more complex than the use of a simple source model and for early design phases could be better to rely on the results of a well known engineering model than in complex calculations, always taking into account the limitations of the model and the uncertainties associated.

In the Proba-3 mission, for which the presented tool has been developed, one of the propulsion subsystems is based on a Hydrazine monopropellant concept. Propulsion supplier has made available information about the undisturbed plume flow of the thrusters and has been implemented a combined source model to adjust the results to the ones provided by the thrusters' supplier. In this way, even with a simplistic engineering model, a good match between the flow fields has been achieved.

In addition, the tool has been developed using a simple geometric approach instead of needing a CAD and a meshing tool to generate the adequate inputs for a N-S or DSMC calculations. Geometry has been modelled as simple surfaces with different basic geometries which are meshed and allow the implementation of a vectorized ray-tracing method using open-source MATLAB® tools.[13]

2. Thrusters' Flow Field

The plume impingement calculations are based in the interaction of the thrusters' plume flow field with the surfaces of the spacecraft. Then for the correct determination of the impingement effects is needed a correct modelling of the flow field. As mentioned previously, there exist complex methods and tools to obtain the most realistic flow field but the present work is more intended to obtain first engineering results accurate enough to perform trade-offs and make preliminary design decisions. Then, the focus is placed on the simple source models that have been used for more than 50 years and perform some tunings on it to obtain a better agreement.

In all the engineering approaches is considered that plume model is not influenced by the presence of the target surface, the expansion of the exhaust gases of the nozzle is considered undisturbed by any surface and then determination of the thermodynamic properties of In the plume is completely independent of the geometry of the impinged surfaces. This hypothesis is widely used and is the base of the SYSTEMA/PLUME® tool.[14] The description of the plume flow field is presented in the following firgure. The following plume model assumptions has been considered in all the relevant

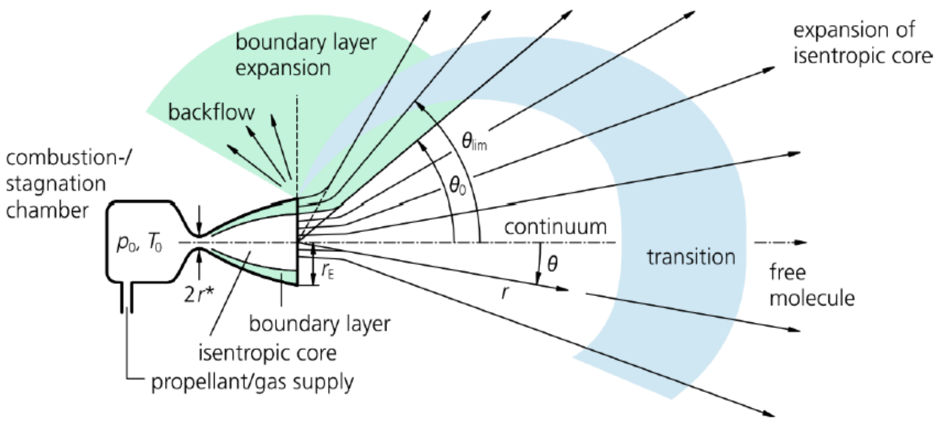

Figure 1: Thruster's Plume Flow expanding to vacuum

literature[13,5,15,16] and will be used for the current study:

- The gas is assumed to have a constant specific heat ratio.
- The impingement occurs at larger distances form the nozzle (more than 4 diameters from the exit nozzle plane).

DOI: 10.13009/EUCASS2019-661

- Continuum regime concept remain valid (molecular flow not considered inside the plume for fluid properties).
- The flow field is divided into two regions separated by a viscous layer: The external atmosphere (vacuum) and the inner region where the jet behaves as in a vacuum expansion.
- The inner region is modelled as an isentropic core up to a determined angle θ_0 meanwhile the expansion region of the boundary layer correspond to a Prandtl-Meyer expansion that cover up to the angle angle $\theta_l im$.
- Inside the isentropic core, streamlines are straight lines emanating from a virtual point centred in the nozzle exit areas.
- Along the streamlines, the local velocity is equal to the limit velocity, being the evolution of properties isentropic.
- The gas is an ideal gas and the flow is chemically frozen,

Considering all of this, and using the cosine law for the description of the flow, the generic equations that determine the density along the plume are:

$$\rho(r,\theta) = A(\rho_* R_*^2/r^2)f(\theta) = \rho(r,0)cos^\kappa\left(\frac{\pi}{2}\frac{\theta}{\theta_{max}}\right), \quad f(\theta) = cos^\kappa\left(\frac{\pi}{2}\frac{\theta}{\theta_{max}}\right); \text{if } \theta < \theta_0 \tag{1}$$

where A is a constant, ρ is gas density at the rocket throat, R_* is throat radius, and θ_{max} and θ_0 are specific angle values chosen by different researchers. A function $f(\theta)$ is introduced in the preceding expression; κ is the so-called beam factor and presents different values in the literature. Boynton[4] noticed that the behaviour away the centerline of the plume was not correctly represented by just the cosine law and proposed an exponential fall function:

$$f(\theta) = f(\theta_0)e^{-\beta(\theta-\theta_0)}; \quad if\theta > \theta_0 \tag{2}$$

where β is a function of the nozzle exit conditions. According to this hypothesis and based on the bibliography consulted, a new source model has been developed based on a combination of two classical source models (Simons model and Mayer model). The aim isr to capture the effects not fully represented in each separate model in order to achieve a better matching with the thruster's plume available information .

2.1 Simons Source Model

This model proposed by Simons and Boynton and modified by other authors like Boetctcher and Legge present a cosine variation for the isentropic core and the modification proposed by Dettlef for the boundary layer expansion follows an exponential function[13515].[16]

$$\rho(r,\theta) = \rho^* A_P \left(\frac{r^{*2}}{r^2 - a\cdot r + b}\right)\cdot g(\theta) \tag{3}$$

$$A_P = \left(\frac{1}{2}\sqrt{\frac{\gamma-1}{\gamma+1}}\right)\frac{1}{\int_0^{\theta_{lim}}\cos^{\frac{2}{\gamma-1}}\left(\frac{\pi\theta}{2\theta_{lim}}\right)\sin\theta d\theta} \tag{4}$$

$$a = 3\theta_e^{1/2}M_e r_e \tag{5}$$

$$b = 5\theta_e M_e^2 r_e^2 \tag{6}$$

The parameters of the equations came from the solution of a bi-dimensional Prandtl-Meyer expansion from the nozzle exit that provide the value of θ_0 and $\theta_l im$.

$$\theta_{lim} = \theta_e + \Delta\theta_{PM}(M_e) - \theta_{BL} \tag{7}$$

The value of the integral of the parameter A_P can be obtained with the boundary layer thickness and the displacement boundary layer thickness as follows.

$$\int_0^{\theta_{lim}}\cos^{\frac{2}{\gamma-1}}\left(\frac{\pi\theta}{2\theta_{lim}}\right)\sin\theta d\theta / \int_0^{\theta_0}\cos^{\frac{2}{\gamma-1}}\left(\frac{\pi\theta}{2\theta_{lim}}\right)\sin\theta d\theta = {}^{(1-\delta_1/r_e)^2}/_{(1-\delta/r_e)^2} \tag{8}$$

While the boundary layer thickness is obtained adjusting the coefficient to match the data provided, different from the ones proposed by Blasius, Pohlhausen or Legge & Boettcher:

$$\delta_e = 10.82 l_e/\sqrt{Re} \tag{9}$$

DOI: 10.13009/EUCASS2019-661

and the boundary layer displacement thickness is the one derived from Karman-Pohlhausen method and a cubic velocity profile:

$$\delta_{e1} = \int_0^{y_1} \left(1 - \frac{u}{U_\infty}\right) = \frac{3}{8}\delta_e \tag{10}$$

The modification of the boundary layer to θ_{lim} came from:

$$\theta_{BL} = \arctan\left[\frac{\delta_e \cos(\theta_e)}{l_e}\right] \tag{11}$$

And the limiting angle of the isentropic core θ_0 is determined by

$$\frac{\theta_0}{\theta_\infty} = \frac{2}{\pi}\cos^{-1}\left\{\left[\left(\frac{2\delta}{R_e}\right) - \left(\frac{\delta}{R_e}\right)^2\right]^{\frac{\gamma-1}{\gamma+1}}\right\} \tag{12}$$

Finally, the functional dependence with the angle $g(\theta)$ is presented as a piecewise function for the different regions, including the exponential decay, as follows:

$$\begin{aligned}
g(\theta) &= \cos^{\frac{2}{\gamma-1}}\left(\frac{\pi\theta}{2\theta_{lim}}\right) && \text{for} \quad \theta < \theta_0 \\
g(\theta) &= \cos^{\frac{2}{\gamma-1}}\left(\frac{\pi\theta_0}{2\theta_{lim}}\right)\exp\left(-c_\rho(\theta - \theta_0)\right) && \text{for} \quad \theta_0 < \theta < \theta_{lim} \\
g(\theta) &= \cos^{\frac{2}{\gamma-1}}\left(\frac{\pi\theta_0}{2\theta_{lim}}\right)\exp\left(-c_\rho(\theta_{lim} - \theta_0)\right) && \text{for} \quad \theta < \theta_{lim}
\end{aligned} \tag{13}$$

where c_ρ is determined in[17] as:

$$c_\rho = A_P \left(\frac{\gamma+1}{\gamma-1}\right)^{\frac{1}{2}} \left(\frac{2\bar{v_{lim}}}{v_{lim}}\right)\left(\frac{r_e}{2\delta}\right)^{\frac{\gamma-1}{\gamma+1}} \tag{14}$$

being the average limit velocity $v_{lim}/2 < \bar{v_{lim}} < v_{lim}$ and the isentropic limit velocity $v_{lim} = \sqrt{\frac{2\gamma}{\gamma-1} \cdot R \cdot T_0}$.

2.2 Mayer Source Model

The Mayer, Hermel and Rogers model is fundamentally the same analytical approach of a source model as Simons' one but change some variables in order to include the thruster performance model via the thruster coefficients and mass flow dependent parameters this formulation contains the effects of nozzle design, and boundary layer momentum and heat transfer lasses ([6,18]). The model considering the boundary layer as another source flow is the following:

$$\rho(r,\theta) = \frac{\alpha_1}{v_{lim} r^2}\left(\cos\frac{\theta}{2}\right)^{\beta_1} + \frac{\alpha_2}{v_{lim} r^2}\left(\cos\frac{\theta}{2}\right)^{\beta_2} \tag{15}$$

$$\beta_1 = 4\frac{C_F(M_e)/C_{F,i}}{1 - C_F(M_e)/C_{F,i}}; \qquad \beta_2 = 4\frac{C_F(M=1)/C_{F,i}}{1 - C_F(M=1)/C_{F,i}};$$

$$\alpha_1 = \left(\dot{W} - \dot{W}_{BL}\right)\frac{(\beta_1 + 2)}{8\pi}; \qquad \alpha_2 = \left(\dot{W}_{BL}\right)\frac{(\beta_2 + 2)}{8\pi}$$

There are two source terms, one due to the main flow and the other that represents the boundary layer flow. The thrust coefficients are defined as:

$$\begin{aligned}
C_{F,i} &= \sqrt{\frac{\gamma^2}{\gamma-1}\left(\frac{2}{\gamma+1}\right)^{\frac{\gamma+1}{\gamma-1}}} \\
\frac{C_F}{C_{F,i}} &= \left(\frac{1+\cos\theta_e}{2}\right)\sqrt{1 - \left(\frac{P_e}{P_0}\right)^{\frac{\gamma-1}{\gamma}}} + \frac{P_e}{P_0}\frac{\epsilon}{C_{F,i}} = \frac{\beta}{\beta+4}
\end{aligned} \tag{16}$$

The parameter ϵ is the nozzle exit area to throat area ratio and can be obtained from the geometry or from the isentropic expansion equations. The boundary layer flow rate can be approximated with the following formula that considers the relationship between the ideal thrust coefficient and the real one. For the analysis the value provided by the thrusters' supplier has been used.

$$\frac{\dot{W}_{BL}}{2\dot{W}} \approx 1 - \frac{C_F}{C_{F,i}} = \frac{4}{\beta+4} \tag{17}$$

DOI: 10.13009/EUCASS2019-661

2.3 Combined Source Model

Considering the two models presented above and the information available from the monopropellant thruster supplier a combined model which gather the best part of the models has been considered.
The model is a simple blending of the two models as both of them have benefits that fit in a better way for each part of the plume. In figure 2 can be seen that there are big differences in the behaviour of the two different source models.

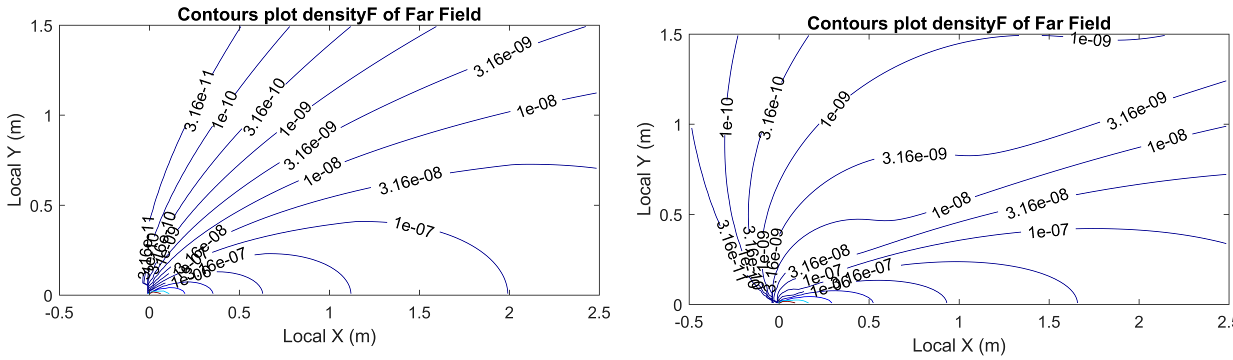

(a) Density Contours Simons Model

(b) Density Contours Mayer Model

Figure 2: **Density Contour Plots for the two different source models used**

Considering the blending function, the combined model is as simple as:

$$\rho = (1 - b)\rho_{Simons} + b\rho_{Mayer}$$

With this approach the and tuning the blending factor b and the other parameters that determine the models, density contours generated are much more close to the ones presented in supplier's information as can be seen in the figure 3.

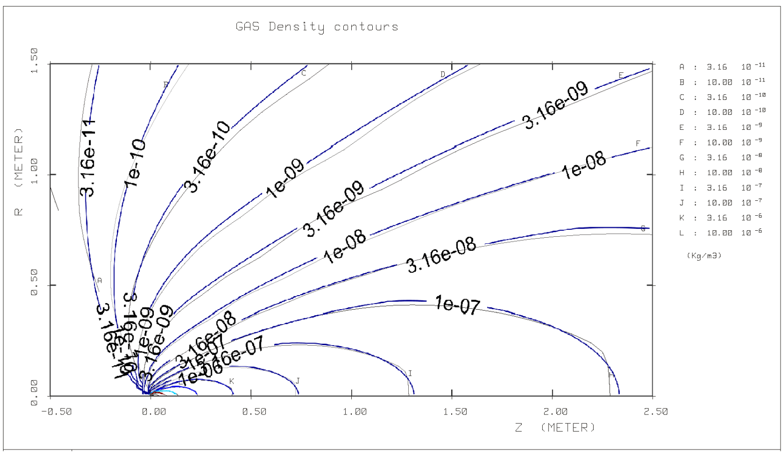

Figure 3: Density Contour Plots for the Combined Source Model

And not only density contours but also the Static Pressure and Temperature ones present a very good match with the information provided by thrusters' supplier as presented in figure 4

This development presents an effective and simple engineering model for the plume flow has been implemented.

3. Geometric Modelling

Once the Thruster's plume flow is obtained, is needed to model the geometry of the spacecraft to determine the plume impingement effects. For that point, with the development done by David Lengland of a MATLAB® library for geometric computing,[13] and the availability of MATLAB® in the company, has been decided to implement the tool in

DOI: 10.13009/EUCASS2019-661

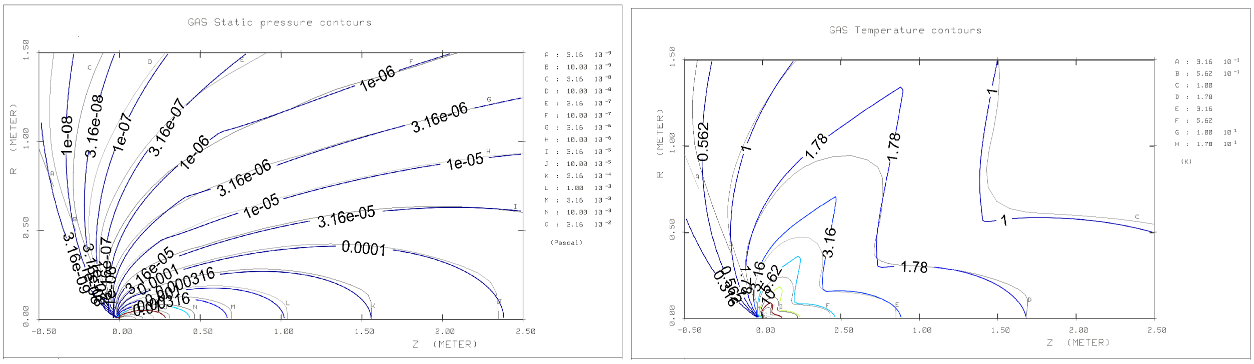

(a) Pressure Contour Plots for the Combined Source Model

(b) Temperature Contour Plots for the Combined Source Model

Figure 4: Pressure and Temperature Contour Plots for the Combined Source Model

MATLAB®.

The geometry calculations are based on simple geometric surfaces to build the complete model. In that way, a basic shapes has been defined (rectangular, circle, triangle) and also taking advantage of the defined functions in Lengland's work[13] , cylinders and spheres are considered basic shapes. The surfaces are meshed and the points are used as end of the rays traced from the thruster's nozzle output. As the source model, or any plume model, depends on the relative position of the surfaces with the thruster's nozzle, is needed to, for each surface that needs to be analysed, calculate this relative position to obtain the flow parameters (pressure, density, temperature, velocity). In addition, to calculate correctly the impingement effects, is needed to perform a shadowing analysis.

The shadow casting is calculated with a ray-tracing method, by connecting all the surfaces' nodes with the source points (thruster's nozzle output) and checking if the generated rays intersect any of the modelled surfaces of the spacecraft. Thanks to the tools used, is not needed to calculate intersections between all the cells with the rays to perform shadow casting. The intersections are mathematically solved when possible reducing the calculations needed and avoiding mesh definition problems.

Based on the first geometry modelling, a GUI tool has been developed in MATLAB® to ease the generation and handling of the geometry.[19] This tool allows an intuitive surface creation that allows to define different parts that can be integrated in the complete model and includes also the definition of the calculation parameters needed for impingement calculations (Surface temperature, reflection coefficients, etc). The figure 5 presents the GUI.
The figures in 6 present the geometry used for the calculations and the cones associated to the thrusters' plume isentropic core to have a first view of the possible impact in the spacecraft surfaces.

4. Impingement Effects

An important issue in the use of any spacecraft propulsion system involves the assessment and reduction of effects caused by the interaction between the thruster plume and spacecraft surfaces. Direct impingement of a thruster plume on surfaces can generate unwanted torques, localized surface heating, and surface contamination. Self-impingement (i.e. the impingement of a thruster plume on a host satellite surface) generally occurs for small surface angles with respect to the propulsion system's thrust vector, or in the thruster backflow.
Following the same approach used in SYSTEMA/PLUME® tool[14] and considers that the flow is in the free-molecular regime. In space, a flow becomes rarefied quickly outside the thruster so this hypothesis matches the reality often.
The calculation of the effects produced by the plume impingement on the spacecraft surfaces, such as:

- Contamination: mass fluxes.
- Dynamic effects: pressure and shear stresses.
- Thermal effects: heat fluxes.

are computed by interpolation of the flow field on the solid surface meshes. The main physical assumption of this method is that the flow is not modified by the solid surfaces so the interaction is calculated directly from the flow prop-

DOI: 10.13009/EUCASS2019-661

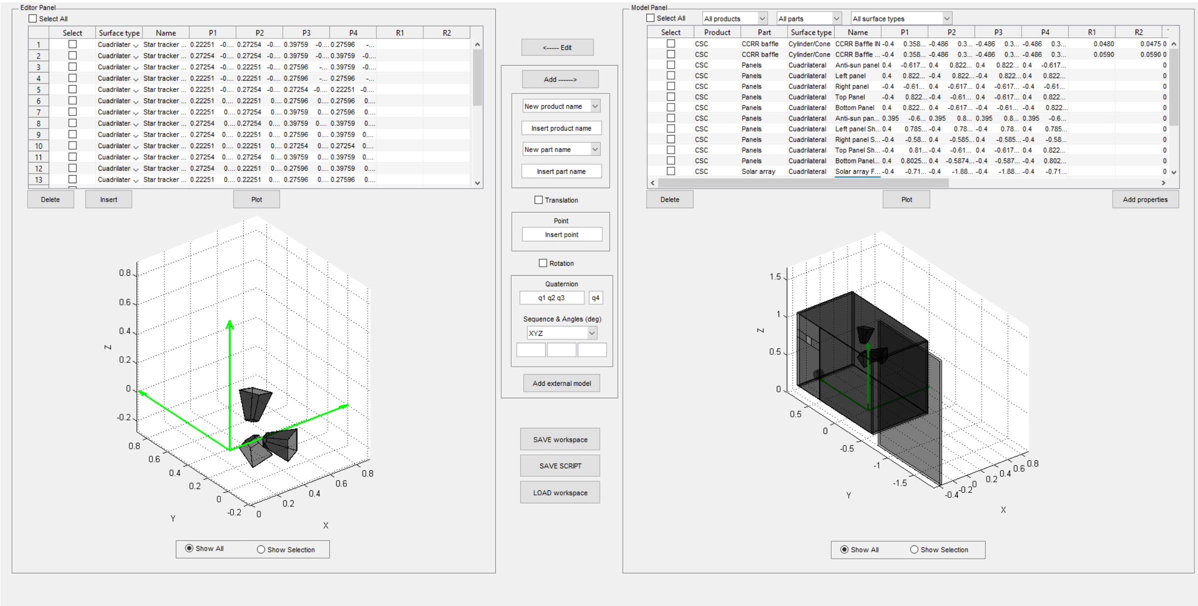

Figure 5: Geometry definition interface

erties predicted. The impingement pressure is the effective force per unit surface applied to the body in the direction normal to the local surface. The pressure applied on the surface is the sum of the pressures due to the incident and reflected gases. Shear stress is the parallel momentum flux to the surface. Like with pressure, the total shear stress τ on the surface is the sum of the incident and reflected shear stresses τ_i and τ_r. The total energy flux is also the sum of the incident and reflected energy fluxes. The incident thermal flux is the sum of the inward translational energy flux and the inward internal energy flux. The thermal flux due to molecules reflected diffusely can be related to the corresponding pressure.

The formulas that provide the forces in the free molecular flow are derived from the Maxwell distribution of velocities corresponding to the thermodynamic state of the molecules. The development of the equations is presented in[14] and.[20]

5. Results

After having modelled the plume flow, the geometry and the adequate equations to model the impingement effects, the tool has been used to perform first fast plume impingement analysis of Proba-3 mission to consider their impact in the thrusters' orientation trade-off analysis. The aim of this paper is to present the tool and only a small part of representative results will be presented.

5.1 Contamination

For the current contamination study there are two main sources of plume impingement contamination: Droplet contamination and Gaseous condensation contamination. Both contamination effects depends on the density of the plume but meanwhile the gaseous contamination depends on the equipment, instruments and radiators temperatures and the capture temperature of the different gaseous species of the plume, the droplet contamination depends more on the droplet flow rate and the gas velocity.

Gaseous contamination

The propellant used in the propulsion system of the spacecaft is Hydrazine (N_2H_4), which is decomposed according to the following main reactions.

$$\begin{aligned} 3N_2H_4 &\rightarrow 4NH_3 + N_2 + 80.15kcal \\ 4NH_3 &\rightarrow 2N_2 + 6H_2 - 44kcal \end{aligned} \tag{18}$$

The capture temperatures for the combustion products are presented in the table below The gaseous products present in the thruster plume will be then NH_3, N_2 and H_2 according to the capture temperatures table the N_2 and H_2 will

DOI: 10.13009/EUCASS2019-661

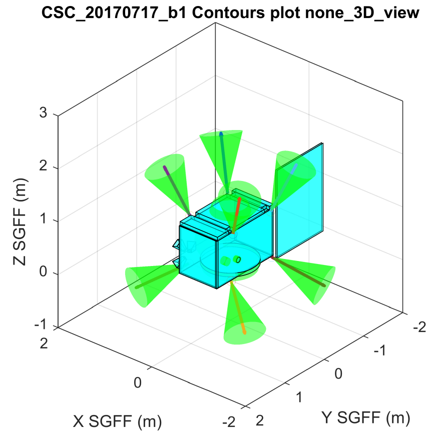

(a) Geometry 3D view

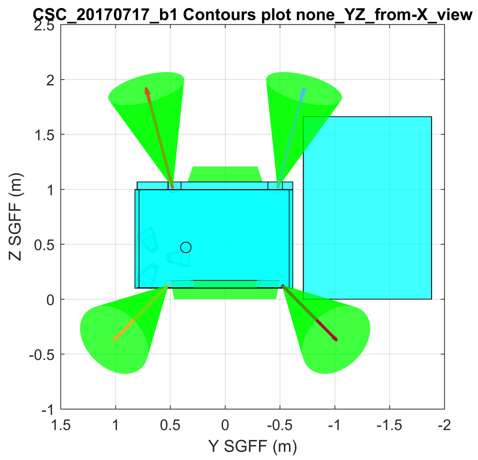

(b) Geometry YZ from-X view

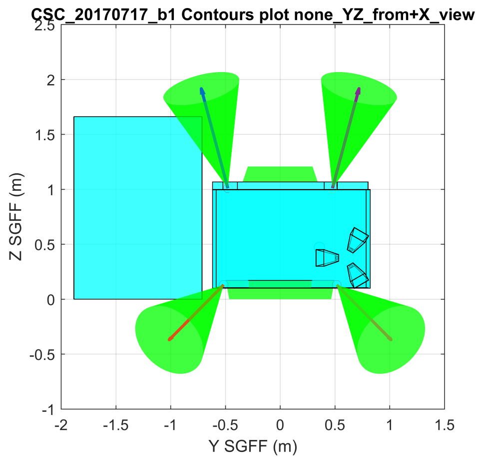

(c) Geometry YZ from+X view

Figure 6: Geometry: spacecraft surfaces and thrusters' isentropic core

Table 1: Capture temperature for different combustion products

Product	Capture Temperature
H_2O	159K
H_2	4K
N_2	26K
NH_3	102K

never condensate as the capture temperatures are $26K$ and $4K$ respectively. The ammonia (NH_3) capture temperature is $102K$, ($-171°C$), which can be reached in some surface during the long eclipse phase. During the cold case, the spacecraft is in safe orbit and only use thrusters for reaction wheel desaturation two hours before entering the eclipse phase so the Sun is illuminating the spacecraft and the temperatures will not fall to the ammonia capture temperature in any surface.

Therefore, with independence of the density, not any surface will be affected by the condensation of gaseous products from the thruster plume and there is no gaseous contamination from the propulsion subsystem.

DOI: 10.13009/EUCASS2019-661

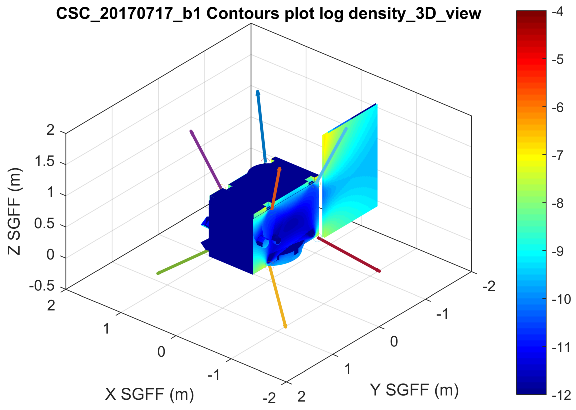

(a) Contours plot log density 3D view

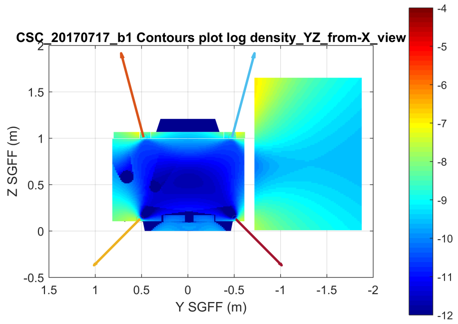

(b) Contours plot log density YZ from-X view

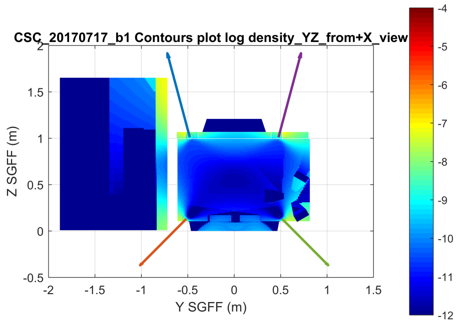

(c) Contours plot log density YZ from+X view

Figure 7: Gas density contours on the spacecraft surfaces

Droplet contamination

Droplets travel in straight lines. Since the sensitive instruments of the mission are isolated with baffles and are not in the direct field of view of the thrusters, no droplet contamination is expected on these instruments. For the contamination in all the surfaces, a safety margin of 100% has been considered due to the nature of the calculations and the complex physics of the problem.

As can be seen in figure 7 the density is very low in all the surfaces of the satellite with a maximum value of $2 \cdot 10^{-7}\ kg/m^3$ in the STR Baffle with lower Z coordinate.

To obtain the droplet contamination is needed to know the droplet ratio of the thruster which represents the percentage of the mass flow rate that are expelled as droplets. With this value and the density and velocity obtained for all the considered surfaces a deposition ratio can be obtained as follows:

$$Deposition\ ratio = Density \cdot Velocity \cdot \cos\alpha \cdot Surface\ Area \cdot Droplet\ ratio \tag{19}$$

The typical droplet ratio of bipropellant thrusters is around 1.5% and monopropellant thrusters generate less droplets so take this value in absence of other data is enough conservative. Where α is the angle between the surface normal and the incident ray of the droplet (the line of sight between the surface point and the thruster nozzle exit). This deposition ratio in kg/s represents the dose of droplets that impact in the surface every second. With the total firing time of the thruster the total deposited mass can be obtained as:

$$Total\ Deposited\ Mass = Deposition\ ratio \cdot Total\ Firing\ time \tag{20}$$

Most droplets will be inside the main flow field, i.e. inside the central cone of $15° - 17°$. But since the amount of droplets in the different parts of the plume is not quantified, the same droplets ratio is assumed outside the main flow

DOI: 10.13009/EUCASS2019-661

field having then a very conservative approach.

The droplets travels in straight line so direct line of sight is needed between the thruster exit and the surface to have any droplet impact. In this way, the droplet contamination of Coronagraph instrument is discarded as there is no direct line of sight from any thruster to the entrance of the tube and also no operation of the thrusters is expected with the CI door opened. As the lenses are deep inside the baffles there is no direct line of sight of the lenses with any thrusters and therefore there is no droplet contamination of the lenses, only of the exterior part of the baffles as can be seen in figure 8

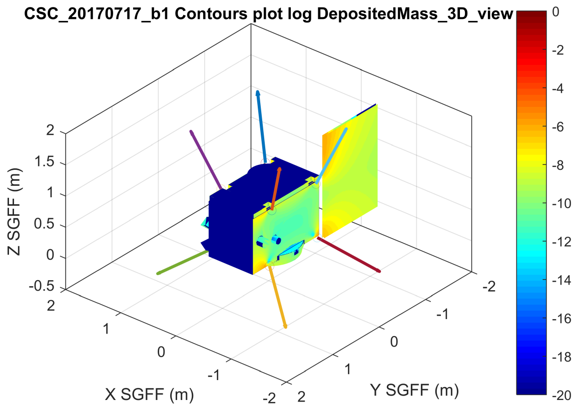

(a) Contours plot log deposited mass 3D view

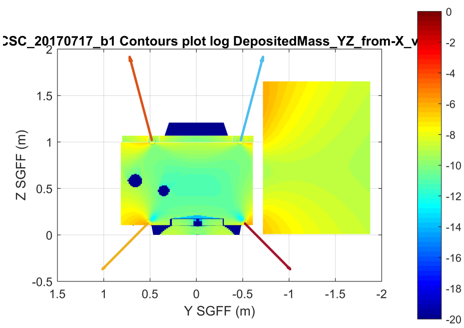

(b) Contours plot log deposited mass YZ from-X view

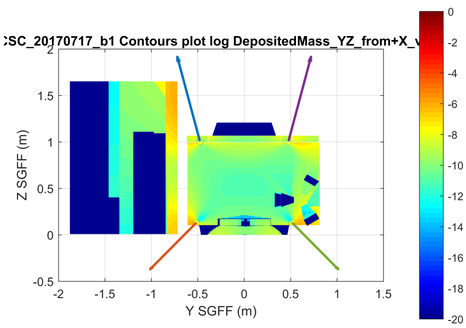

(c) Contours plot log deposited mass YZ from+X view

Figure 8: Deposited mass contours on the spacecraft surfaces

5.2 Perturbation Forces and Torques

Two worst-case scenarios have been considered and simulated for:

- WC1 considers that all incident molecules which are specular reflected ($\epsilon = 1$). The tangential interaction coefficient is 0 and the normal interaction coefficient is 2. This means that the surface receives no tangential force component and that the pressure on the surface is at its maximum value.
- WC2 considers that all incident molecules which are diffusely reflected ($\epsilon = 0$). The tangential interaction is 1 and the normal interaction coefficient is 1.

Both WC scenarios are theoretical WC and are therefore more conservative than what will be experienced in practice which will be an intermediate situation in which the incident molecules are reflected a fraction in specular way and the rest in a diffuse way.

Tables 2 and 3 present the disturbance forces and torques in the spacecraft reference frame.

DOI: 10.13009/EUCASS2019-661

Table 2: Disturbing Forces generated by the different thrusters

	Worst Case 1 Impingement Forces (Nm)			Worst Case 2 Impingement Forces (Nm)		
	Force_x	Force_y	Force_z	Force_x	Force_y	Force_z
CPR_THR1A	-3.049E-12	-9.819E-13	-2.605E-9	-2.274E-11	-4.909E-13	-1.303E-9
CPR_THR2A	1.224E-8	3.169E-7	-3.8141E-7	6.1200E-9	1.585E-7	-1.907E-7
CPR_THR3A	-1.6649E-8	8.893E-9	-8.301E-9	-1.168E-8	4.449E-9	-4.143E-9
CPR_THR4A	1.817E-8	3.132E-8	-3.376E-8	9.086E-9	1.566E-8	-1.688E-8
CPR_THR5A	-2.286E-6	2.023E-6	1.332E-6	-1.146E-6	1.013E-6	6.6519E-7
CPR_THR6A	1.882E-5	-1.029E-6	1.980E-5	9.152E-6	-4.742E-7	9.8316E-6
CPR_THR7A	-1.478E-7	4.618E-8	-4.18403E-8	-7.908E-8	2.300E-8	-2.121E-8
CPR_THR8A	4.944E-7	3.797E-7	6.4550E-8	2.486E-7	1.898E-7	3.177E-8

Table 3: Disturbing Torques generated by the different thrusters

	Worst Case 1 Impingement Torques (Nm)			Worst Case 2 Impingement Torques (Nm)		
	Torque_x	Torque_y	Torque_z	Torque_x	Torque_y	Torque_z
CPR_THR1A	2.565E-10	-1.159E-9	-1.525E-12	1.283E-10	-6.125E-10	-2.756E-11
CPR_THR2A	-4.563E-7	2.051E-7	1.556E-7	-2.281E-7	1.025E-7	7.779E-8
CPR_THR3A	-8.518E-9	-1.275E-8	5.895E-9	-4.255E-9	-1.134E-8	-2.368E-9
CPR_THR4A	-2.645E-8	2.366E-8	8.871E-9	-1.323E-8	1.183E-8	4.436E-9
CPR_THR5A	-2.498E-7	-5.776E-7	4.471E-7	-1.263E-7	-2.899E-7	2.234E-7
CPR_THR6A	1.157E-5	-4.935E-6	-1.313E-5	5.733E-6	-2.467E-6	-6.373E-6
CPR_THR7A	-2.939E-8	-3.693E-8	-3.377E-9	-1.468E-8	-1.933E-8	-7.662E-9
CPR_THR8A	-1.001E-7	1.011E-7	3.797E-8	-5.016E-8	5.087E-8	1.902E-8

5.3 Heat Transfer

As the spacecraft thrusters are expelling Hydrazine decomposed at a very high speeds, the elements near the plume area can receive thermal load due to the friction of the gas. In order to consider the worst case possible is supposed that the reflection from all surfaces is completely diffuse and there is complete thermal accommodation of the particles. Considering this, the heat flux of the impingement plume into the different surfaces is presented in the figure 9

6. Conclusion

This paper presented an efficient approach to execute a Plume Impingement analysis without the need of third party tools using an in-house development approach. The developed tool has set the basis for the generation of a System wide framework for platform analysis in which has been already integrated.

The validity of the calculations shall be identical to the commercial tool SYSTEMA/PLUME® in terms of the impingement effects calculation as is based directly in the formulation used to implement this commercial tool from Airbus: to consider the flow undisturbed by the surfaces and free molecular flow interactions.[14] The validity of the flow calculations is also justified as uses has been performed using a modified source model that perfectly fits the results provided by Monopropellant thrusters' supplier and is in line with ECSS recommendations and literature for plume impingement analysis.[1]

The developed tool has been used to perform a first trade-off selection between different thrusters' orientation orientations and to successfully perform the Plume Impingement analysis of Proba-3 In Orbit Demonstrator mission evaluating Contamination effects, Disturbing Forces and Torques, Heat fluxes and possible blinding effects on Star Trackers due to the firing of the thrusters, helping to select the most adequate configuration for the system considering all the possible impacts on the mission performances .

Even if for this study has been implemented a simple source model for the plume modelling, in[21] is presented a comparison between the new methods and the classic source model based on Simmons[3] approach and the difference

DOI: 10.13009/EUCASS2019-661

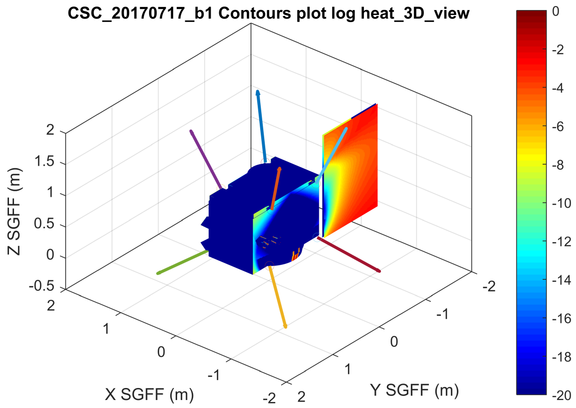

(a) Contours plot log deposited mass 3D view

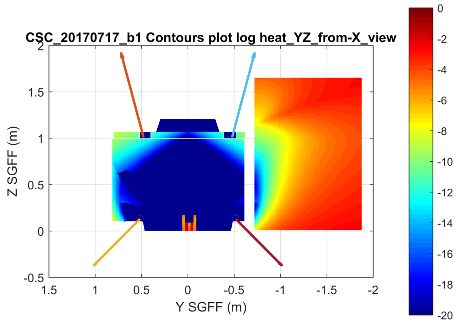

(b) Contours plot log deposited mass YZ from-X view

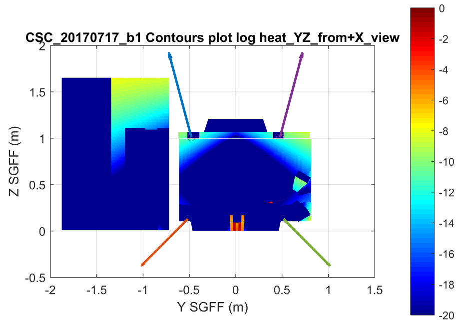

(c) Contours plot log deposited mass YZ from+X view

Figure 9: Heat transfer contours on the spacecraft surfaces

is not so great to invalidate the calculations if the adequate margins are taken. In addition, the generated tool is able to integrate other very promising approaches as the ones from the gaskinetic theory[11,12] and get much more accurate results in line with the state-of-the-art plume flow calculations.

7. Acknowledgments

This work has been developed in the frame of Proba-3 European Space Agency's In Orbit Demonstration mission at SENER Aeroespacial.

References

[1] George Dettleff. Plume flow and plume impingement in space technology. *Progress in Aerospace Sciences*, 28(1):1 – 71, 1991.

[2] Rhonald M. Jenkins, Alessandro Ciucci, and John E. Cochran. Simplified model for calculation of backflow contamination from rocket exhausts in vacuum. *Journal of Spacecraft and Rockets*, 31(2):265–270, 1994.

[3] G. A. SIMONS. Effect of nozzle boundary layers on rocket exhaust plumes. *AIAA Journal*, 10(11):1534–1535, 1972.

[4] F. P. BOYNTON. Exhaust plumes from nozzles with wall boundary layers. *Journal of Spacecraft and Rockets*, 5(10):1143–1147, 1968.

[5] I. D. Boyd and J. P. W. Stark. Modification of the simons model for calculation of nonradial expansion plumes. *Progress in Astronautics and Aeronautics*, 116:327–339, 1989.

DOI: 10.13009/EUCASS2019-661

[6] E. MAYER, J. HERMEL, and A. W. ROGERS. Thrust loss due to plume impingement effects. *Journal of Spacecraft and Rockets*, 23(6):554–560, 1986.

[7] G. A Bird. *Molecular gas dynamics and the direct simulation of gas flows*. Oxford : Clarendon Press, repr. (with corrections) edition, 1995.

[8] G. A Bird. *The DSMC method*. [U.S.] : [CreateSpace], version 1.2 edition, 2013.

[9] Michael Woronowicz. Development of a novel free molecule rocket plume model. *AIP Conference Proceedings*, 585(1):798–805, 2001.

[10] Michael Woronowicz. Further studies using a novel free molecule rocket plume model. *AIP Conference Proceedings*, 663(1):588–595, 2003.

[11] Chunpei Cai and Iain D. Boyd. Collisionless gas expanding into vacuum. *Journal of Spacecraft and Rockets*, 44(6):1326–1330, 2007.

[12] Chunpei Cai. Rocket plume modeling. *AIAA Journal*, 52(12):2907–2910, 2014.

[13] David Lengland. Matgeom.

[14] M. Warttelski. Simulation of plume-spacecraft interaction. Master's thesis, Royal Institute of Technology, Stockholm, Sweden, 2009.

[15] Georg Dettleff and Martin Grabe. *Basics of Plume Impingement Analysis for Small Chemical and Cold Gas Thrusters*, pages 1–40. Models and Computational Methods for Rarefied Flows. RTO/NATO, 2011. Papers presented during the AVT-194 RTO AVT/VKI Lecture Series held at the von Karman Institute, CD-ROM, Paper 12.

[16] Iain D. Boyd. *Modelling of satellite control thruster plumes*. PhD thesis, University of Southampton, October 1988.

[17] H. Legge and R.-D. Boettcher. *Modelling Control Thruster Plume Flow and Impingement*, volume 2, pages 983–992. Springer US, 1985.

[18] E. MAYER and R. PRICKETT. Rocket plume impingement heat transfer on plane surfaces. *Journal of Spacecraft and Rockets*, 24(4):291–295, 1987.

[19] S. Madrid. Development of a suite of interdisciplinary tools for concurrent design of space missions. Master's thesis, Universidad Carlos III, Madrid, Spain, 2018.

[20] LEE H. SENTMAN. Free molecule flow theory and its application to the determination of aerodynamic forces. page 111, 10 1961.

[21] Chunpei Cai. A gaskinetic model for planar plume and comparisons with the simons plume model. *Frontiers in Aerospace Engineering*, 2(1):67–72, 2013.